

Supporting Information

Catalytic Systems Based on Chromium(III)

Silylated-Diphosphinoamines for Selective Ethylene Tri-/Tetramerization

Fakhre Alam,[†] Le Zhang,^{†,‡} Wei Wei,[†] Jiadong Wang,[†] Yanhui Chen,[†] Chunhua Dong,^{,‡} Tao
Jiang^{*,†}*

[†]College of Chemical Engineering and Material Science, Tianjin University of Science and
Technology, Tianjin 300457, China

[‡]Handan Key Laboratory of Organic Small Molecule Materials, Handan University, Handan
056005, China

Corresponding Authors

*E-mail: jiangtao@tust.edu.cn

*E-mail: dongchunhua@iccas.ac.cn

1 Experimental Section

1.1 General information:

All procedures were carried out in oven dried flasks under N₂ atmosphere using standard Schlenk technique or purified N₂-filled glovebox. Anhydrous solvents were obtained using multi-column purification system, while all reagents were purchased from Aldrich and used as received. NMR spectra were recorded by Bruker Ascend^{III}-400 (400 MHz for ¹H, 162 MHz for ³¹P and 101 MHz for ¹³C in C₆D₆) at 300K. Lithium salts of diphenylphosphanamine were prepared by simple lithiation of corresponding diphenylphosphanamine,¹ while Chlorodimethyl((diphenylphosphino)methyl) silane was prepared by already reported methods.²

1.2 Preparation of Ligands

The ligands **L¹-L⁵** were prepared by simple salt metathesis reactions, the detail procedure is given below.

N-cyclopentyl-N-(((diphenylphosphanyl)methyl)dimethylsilyl)-1,1-diphenylphosphanamine (L¹)

To a solution of lithium cyclopentyl(diphenylphosphanyl)amide (0.47 g, 1.70 mmol) in n-hexane at -35 °C was added Chlorodimethyl((diphenylphosphino)methyl)silane (0.5 g, 1.70 mmol,) under stirring. The stirring was continued overnight at room temperature and then filtered the reaction mixture to remove lithium chloride salt. The solution was vacuum dried, washed with n-hexane (3x10 mL) and dried again under vacuum. The **L¹** was isolated after recrystallization in hexane at -35 °C in 75% yield. ¹H NMR (C₆D₆): δ 0.27 (s, 6H), 1.43–1.62 (m, 8H), 1.80 (s, 2H), 3.59–3.67 (m, 1H), 7.01–7.67 (m, 20H). ³¹P NMR (C₆D₆) δ (-22.62)–(-22.58) (d), 46.49 (br, s). ¹³C NMR (C₆D₆) δ 2.96, 3.04, 17.50, 17.60, 17.83, 17.92, 22.69, 34.13, 34.18,

61.36, 128.06, 128.12, 128.17, 128.21, 128.27, 131.97, 132.17, 132.57, 132.77, 140.41, 140.59, 141.61, 141.77.

N-(2,6-diisopropylphenyl)-N-(((diphenylphosphanyl)methyl)dimethylsilyl)-1,1-diphenylphosphanamine (L²)

The preparation procedure for **L²** was same as for **L¹** except that lithium (2,6-diisopropylcyclohexyl)(diphenylphosphanyl)amide (0.59 g, 1.60 mmol) was used in 1:1 with Chlorodimethyl((diphenylphosphino)methyl)silane (0.46 g, 1.60 mmol). The ligand was isolated after recrystallization in 87% yield. ¹H NMR (C₆D₆): δ 0.30 (s, 6H), 0.64–0.66 (d, 6H), 1.15–1.16 (d, 6H), 1.88 (s, 2H), 3.47–3.54 (m, 2H), 7.00–7.63 (m, 23H). ³¹P NMR (C₆D₆) δ (-21.21)–(-21.18) (d), 52.88–52.92 (d). ¹³C NMR (C₆D₆) δ 2.86, 2.91, 2.95, 17.62, 18.00, 24.49, 25.51, 28.90, 124.74, 126.50, 128.42, 128.58, 128.65, 129.35, 132.95, 133.15, 135.01, 135.25, 139.52, 139.74, 141.84, 141.00, 143.05, 147.98, 148.01.

N-(((diphenylphosphanyl)methyl)dimethylsilyl)-N-isopropyl-1,1-diphenylphosphanamine (L³)

The preparation procedure for **L³** was the same as for **L¹** except that lithium(diphenylphosphanyl)(isopropyl)amide (1.2 g, 4.8 mmol) was used in 1:1 with Chlorodimethyl((diphenylphosphino)methyl)silane (1.40 g, 4.8 mmol). The ligand was isolated as a white solid after recrystallization in 71% yield. ¹H NMR (C₆D₆): δ 0.15 (s, 6H), 0.96–0.97 (d, 6H), 1.53 (s, 2H), 3.19–3.26 (m, 1H), 7.02–7.48 (m, 20H). ³¹P NMR (C₆D₆) δ -24.50 (s), 34.79 (s). ¹³C NMR (C₆D₆) δ 0.22, 0.25, 15.52, 15.83, 23.46, 23.53, 45.95, 46.17, 125.76, 125.82, 125.95, 126.02, 126.17, 128.75, 128.95, 129.94, 130.15, 130.35, 132.13, 132.26, 137.93, 138.08, 141.07, 141.20.

N-cyclopentyl-1-((diphenylphosphanyl)methyl)-N(((diphenylphosphanyl)methyl)dimethylsilyl)-1,1-dimethylsilanamine (L⁴)

To 50 mL THF solution of 1-equivalent cyclopentylamine (0.24 g, 2.85 mmol) and 2-equivalent Et₃N (0.8 mL, 5.64 mmol) was slowly added a 20 mL THF solution of 2-equivalent Chlorodimethyl((diphenylphosphino)methyl)silane (1.65 g, 5.64 mmol) at room temperature under stirring and continuously stirred for overnight. After filtration, the removal of THF was carried out under vacuum; hexane was added and again the reaction mixture was filtered to ensure the removal of trimethylaminehydrochloride salt. A colorless oil was collected in n-hexane and dried under vacuum to get **L⁴** in 80% yield with more than 96% purity based on ³¹P NMR. ¹H NMR (C₆D₆): δ 0.06 (s, 6H), 0.14 (d, 6H), 1.03–1.10 (m, 2H), 1.33 (s, 2H), 1.36–1.41 (m, 2H), 1.53 (s, 4H), 1.67–1.75 (m, 2H), 3.06–3.16 (m, 1H), 7.02–7.51 (m, 20H). ³¹P NMR (C₆D₆) δ -25.15 (s), -22.86 (s). ¹³C NMR (C₆D₆) δ 0.27, 0.31, 2.52, 2.55, 15.40, 15.71, 17.84, 18.15, 23.29, 37.37, 53.79, 128.08, 128.09, 128.16, 128.24, 128.31, 128.46, 132.04, 132.23, 132.44, 132.56, 132.64, 132.76, 133.85, 134.01, 140.24, 140.39, 141.86, 142.02.

1-((diphenylphosphanyl)methyl)-N-(((diphenylphosphanyl)methyl)dimethylsilyl)-N-isopropyl-1,1-dimethylsilanamine (L⁵)

The preparation procedure for **L⁵** was the same as for **L⁴**, except that 2-equivalent of Chlorodimethyl((diphenylphosphino)methyl)silane (1.67 g, 5.7 mmol) was used with 2-equivalent of Et₃N (0.8 mL, 5.64 mmol) and 1-equivalent of isopropylamine (0.16 g, 2.85 mmol). Furthermore, the product obtained was a colorless oil in 75% yield with more than 96% purity based on ³¹P NMR. ¹H NMR (C₆D₆): δ 0.03 (s, 7H), 0.15 (s, 5H), 0.93 (s, 3H), 0.95 (s, 3H), 1.31 (s, 3H), 1.53 (s, 1H), 2.87–2.95 (m, 1H), 7.02–7.51 (m, 20H). ³¹P NMR (C₆D₆) δ -24.45 (s), -22.14 (s). ¹³C NMR (C₆D₆) δ 0.13, 0.18, 0.19, 0.22, 1.63, 2.40, 15.32, 15.63, 17.69,

18.00, 27.55, 29.66, 42.35, 42.78, 127.27, 127.51, 127.75, 127.92, 127.94, 128.00, 131.88, 132.07, 132.28, 132.40, 132.48, 132.60, 132.76, 140.08, 140.23, 141.68, 141.84.

1.3 Synthesis of Precatalysts (1-5). **[L¹(CrCl₃(THF)) (1).** To a CH₂Cl₂ solution of **Ph₂PN(cyclopentyl)Si(CH₃)₂CH₂PPh₂ (L¹)** (0.36 g, 0.68 mmol) was added **CrCl₃(THF)₃** (0.24 g, 0.64 mmol) and stirred for 2h at room temperature. The solvent was vacuum evaporated and 15 mL of hexane was added to the reaction mixture for complete precipitation. The product was filtered, washed with hexane (3×10 mL) and vacuum dried to yield **1** as a green powder in 85% yield. Anal. Calcd for C₃₆H₄₅Cl₃CrNOP₂Si (%): C, 57.18; H, 6.00; N, 1.85.

[L²(CrCl₃(THF)) (2). Precatalyst **2** was prepared via similar procedure as used for **1**. The product was obtained as a brown powder in 85% yield. Anal. Calcd for C₄₃H₅₉Cl₃CrNOP₂Si (%): C, 60.45; H, 6.96; N, 1.64.

[L³(CrCl₃(THF)) (3). Precatalyst **3** was prepared via similar procedure as used for **1**. The product was obtained as a green powder in 90% yield. Anal. Calcd for C₃₄H₄₃Cl₃CrNOP₂Si (%): C, 55.93; H, 5.94; N, 1.92.

[L⁴(CrCl₃(THF)) (4). Precatalyst **4** was prepared via similar procedure as used for **1**. The product was obtained as a green powder in 70% yield. Anal. Calcd for C₃₅H₄₅Cl₃CrNP₂Si₂ (%): C, 55.59; H, 6.00; N, 1.85.

[L⁵(CrCl₃(THF)) (5). Precatalyst **5** was prepared via similar procedure as used for **1**. The product was obtained as a green powder in 75% yield. Anal. Calcd for C₃₃H₄₃Cl₃CrNP₂Si₂ (%): C, 54.28; H, 5.94; N, 1.92.

Synthesis of [Cr(CO)₄(L²)] complex (6); (L² = Ph₂P(2,6-diisopropylphenyl)N(CH₃)₂SiCH₂PPh₂)

A round bottom flask was charged with Cr(CO)₆ (0.08 g, 0.38 mmol) and **L²** (0.20 g, 0.32 mmol) before the toluene (50 mL) was added. The mixture was refluxed for 48 hours, during

which the solution turned yellow and then cooled to room temperature. The solution was filtered and the toluene was removed under vacuum to get a yellow solid. The yellow solid was triturated from hexane to get a white color complex and vacuum dried. The complex was dissolved in minimum amount of DCM and slowly layered with hexane and stored at -35 °C to get single crystals of **6**.

1.4 Ethylene Oligomerization

Transparent glass autoclave reactor (150 mL) equipped with a stirrer and temperature probing device was used for selective ethylene oligomerization. Under a N₂ atmosphere, the catalyst was injected into the reactor followed by pressurized ethylene and run the reaction for 30 min. the reactor was depressurized and cooled up to 0 °C using an ice bath and then quenched by using 50 mL 10% MeOH and HCl. The organic phase was separated and analyzed by GC-FID (gas chromatography with flame ionization detector) using Agilent 6890 with HP-5 GC capillary column, while heptane was used as an internal standard.

2 NMR Spectra of Ligands L¹-L⁵

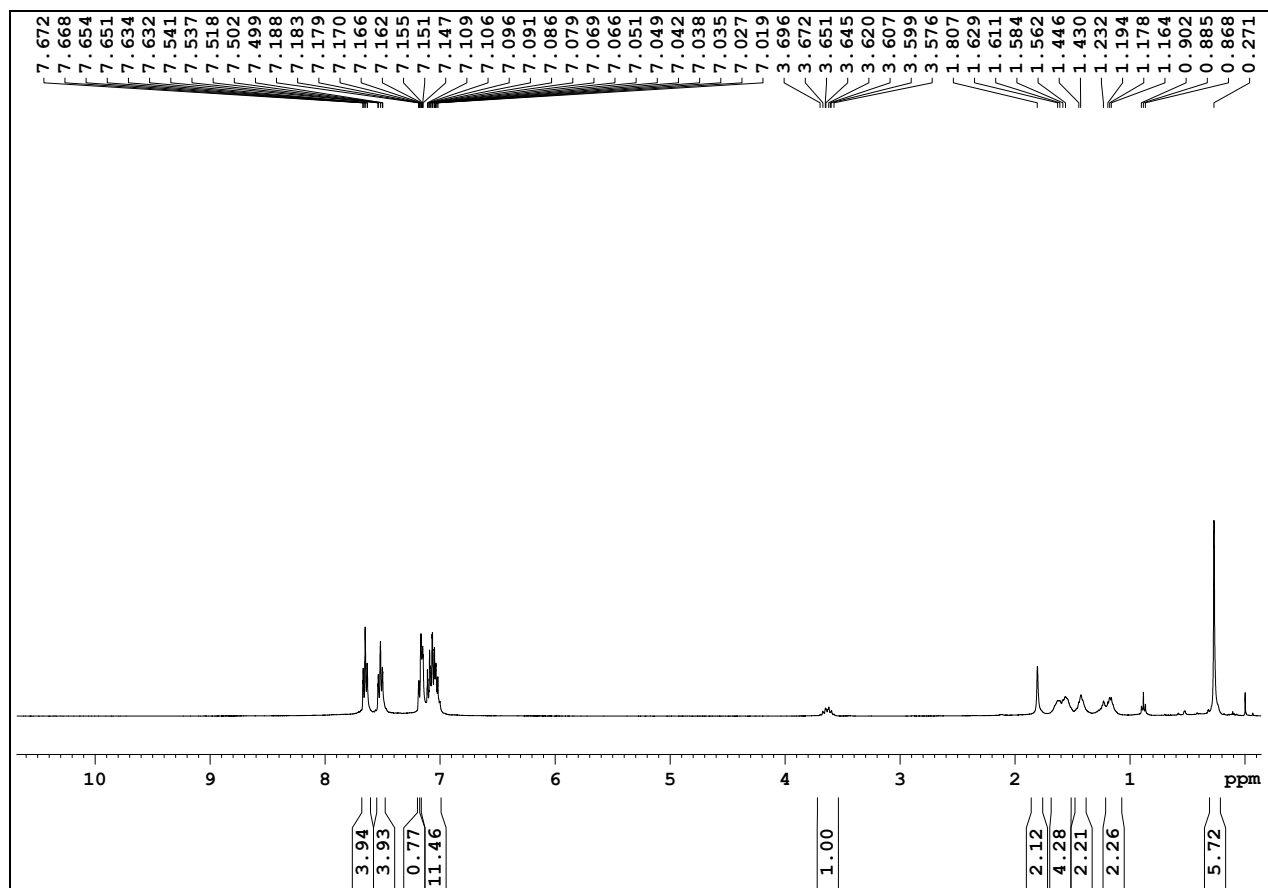


Figure S1. ¹H NMR Spectrum of L¹

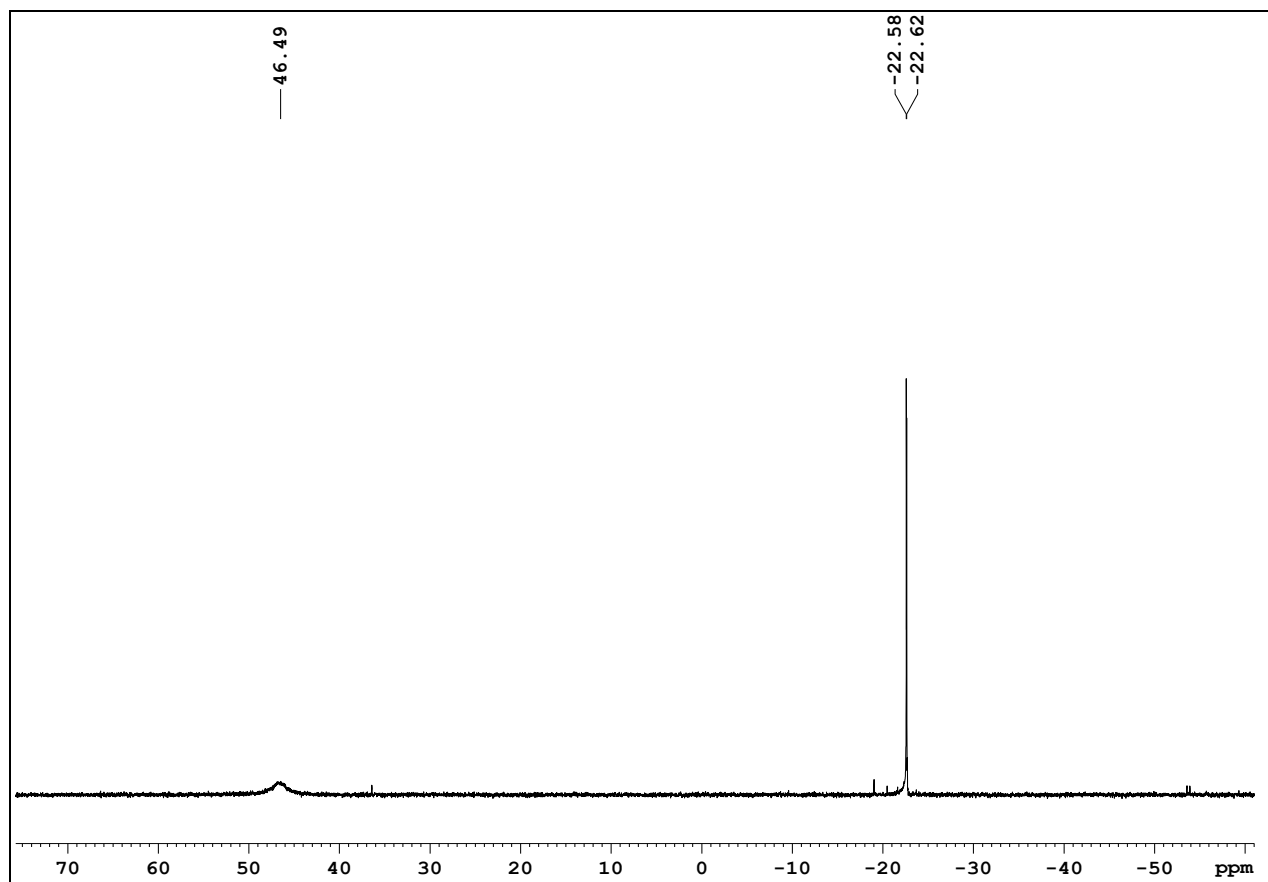


Figure S2. ^{31}P NMR Spectrum of L^1

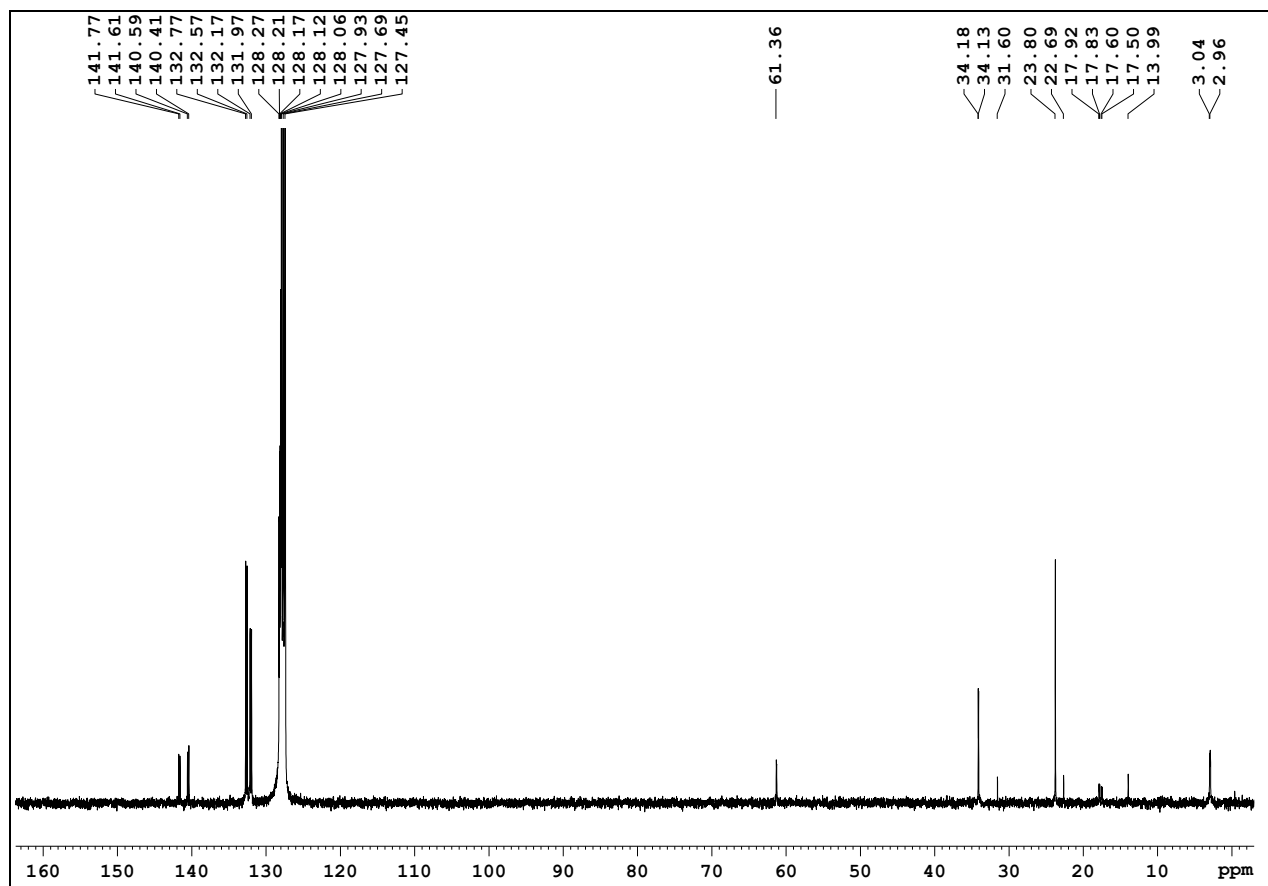


Figure S3. ^{13}C NMR Spectrum of L^1

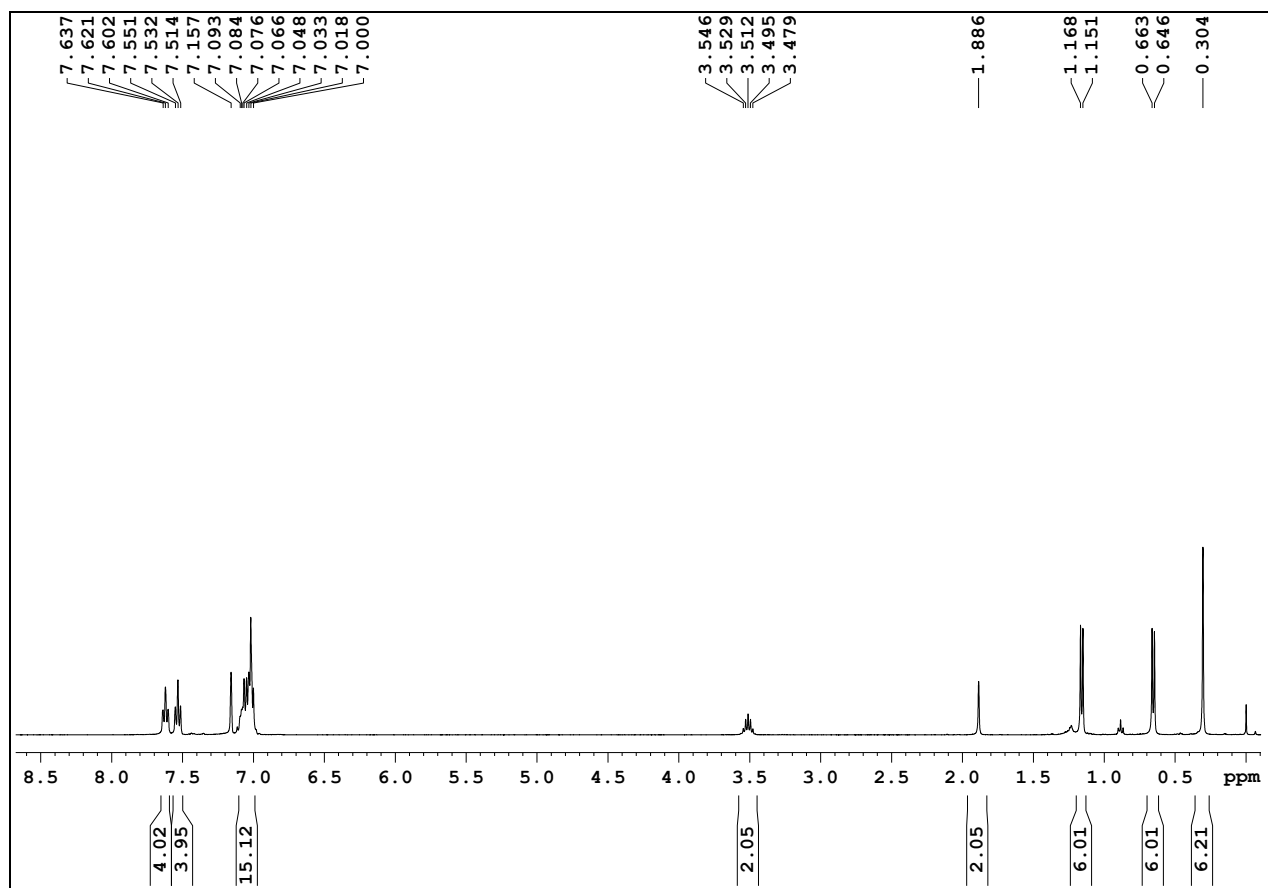


Figure S4. ^1H NMR Spectrum of L^2

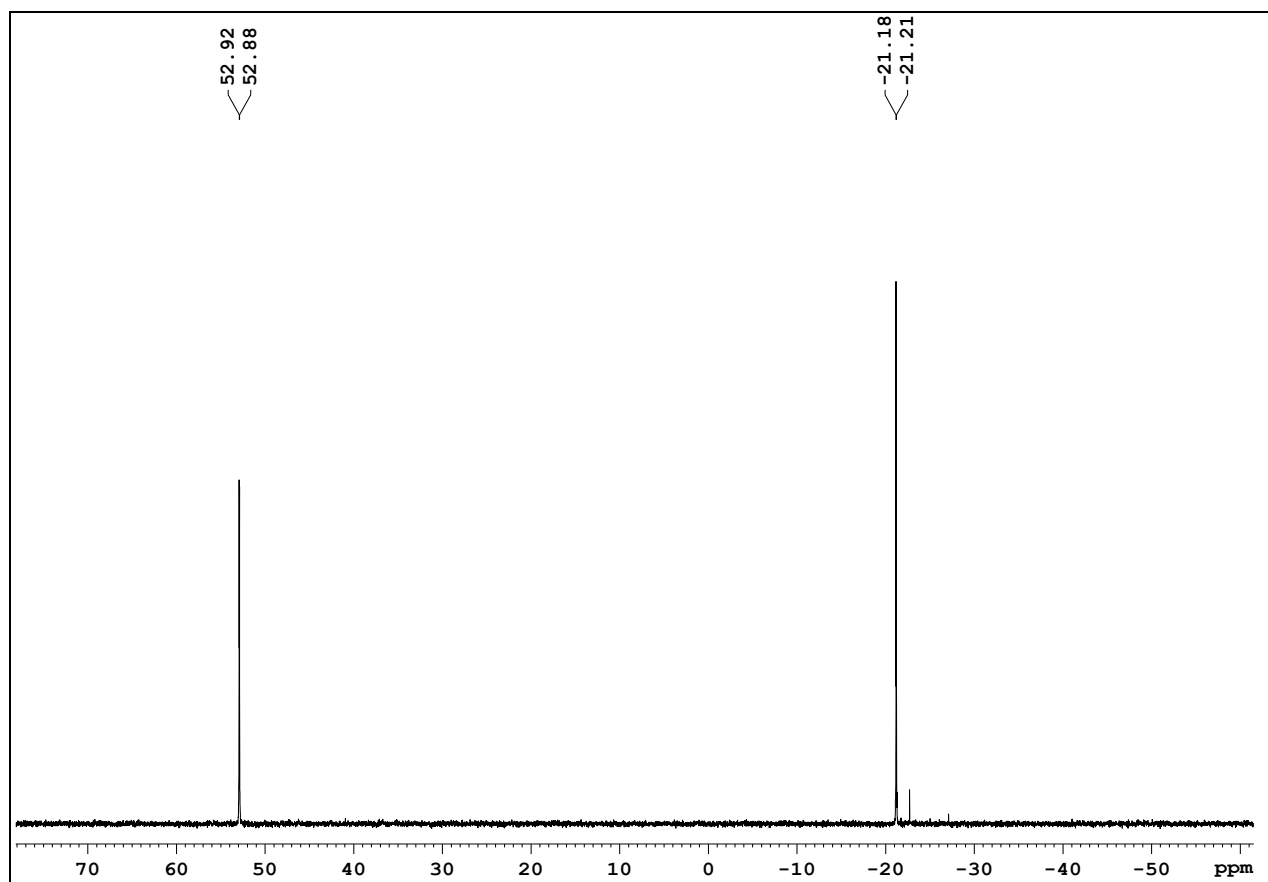


Figure S5. ^{31}P NMR Spectrum of L^2

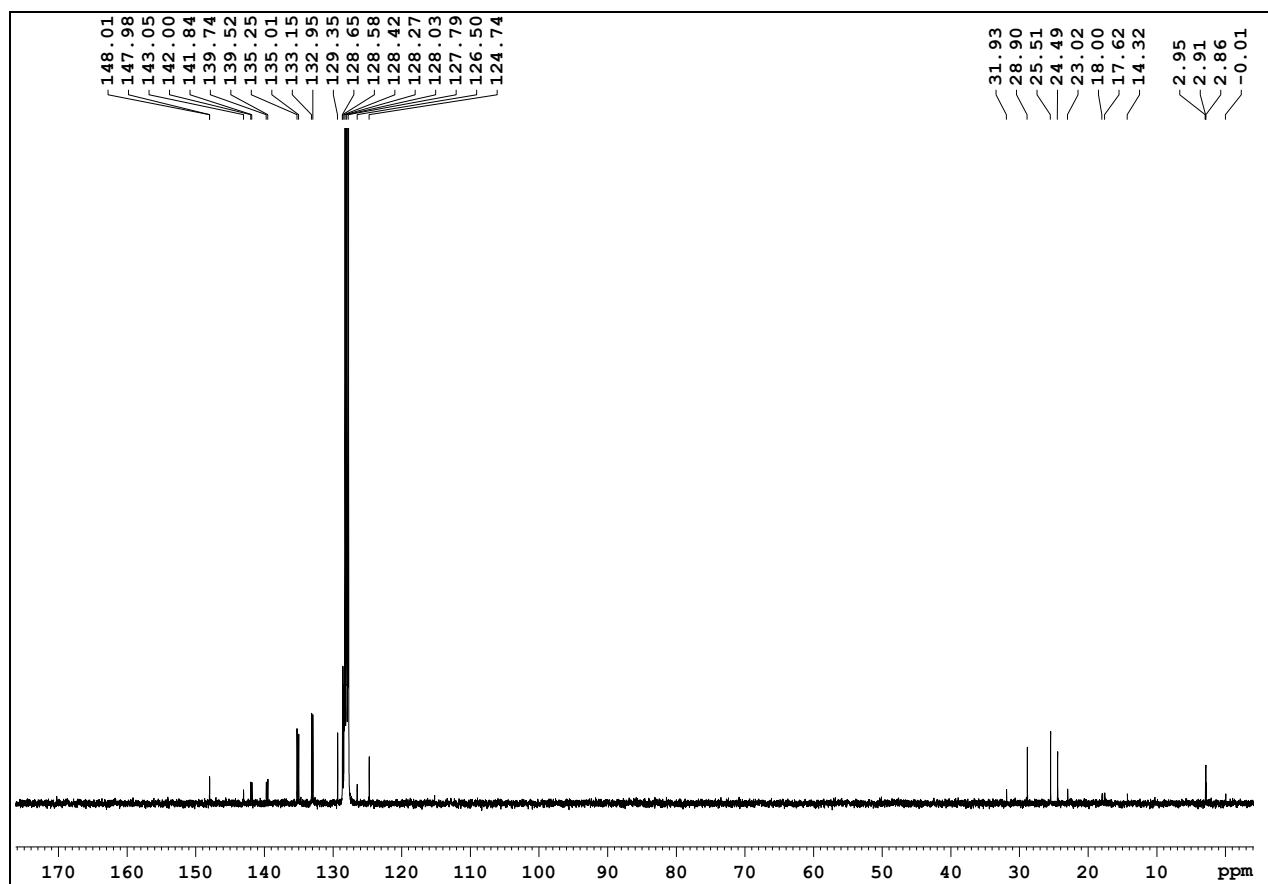


Figure S6. ¹³C NMR Spectrum of L^2

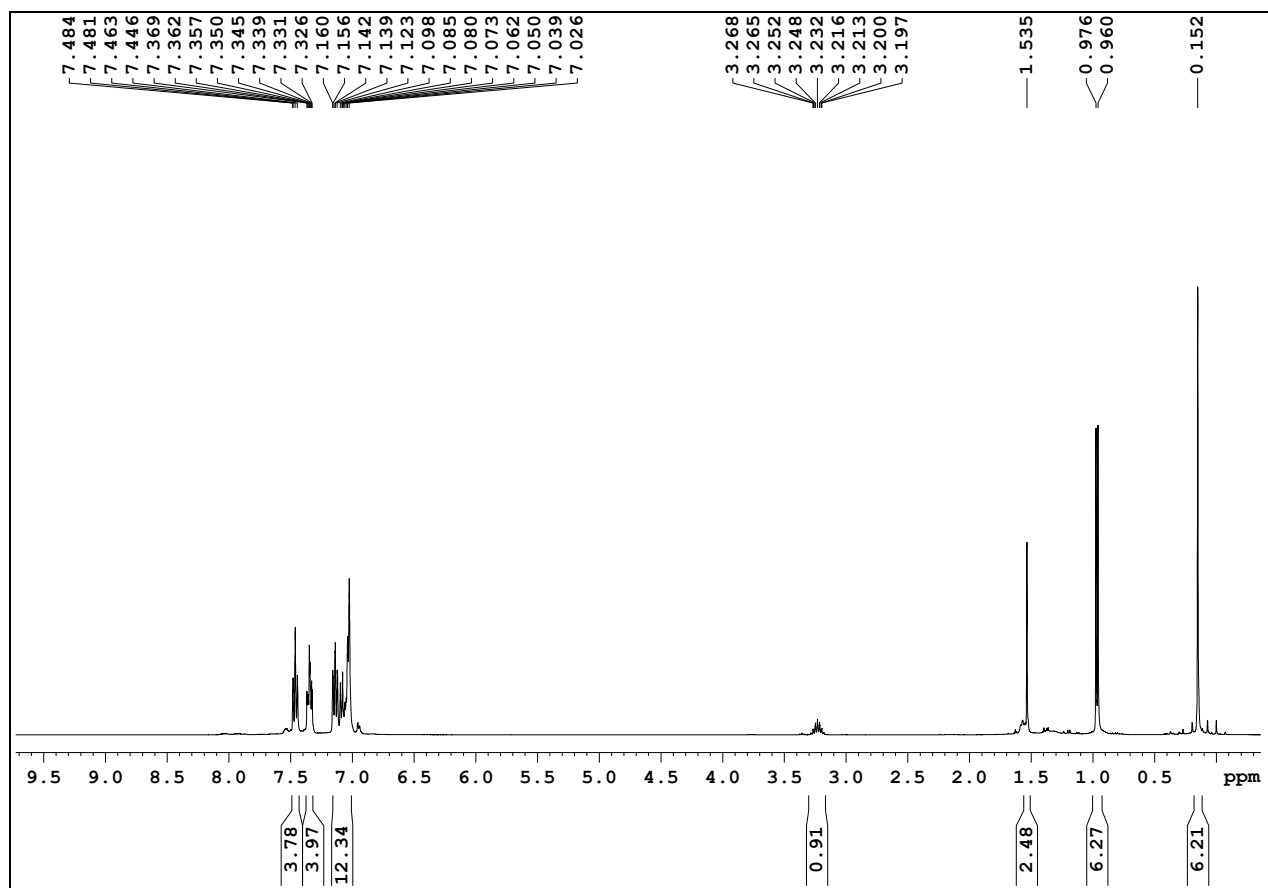


Figure S7. ^1H NMR Spectrum of L^3

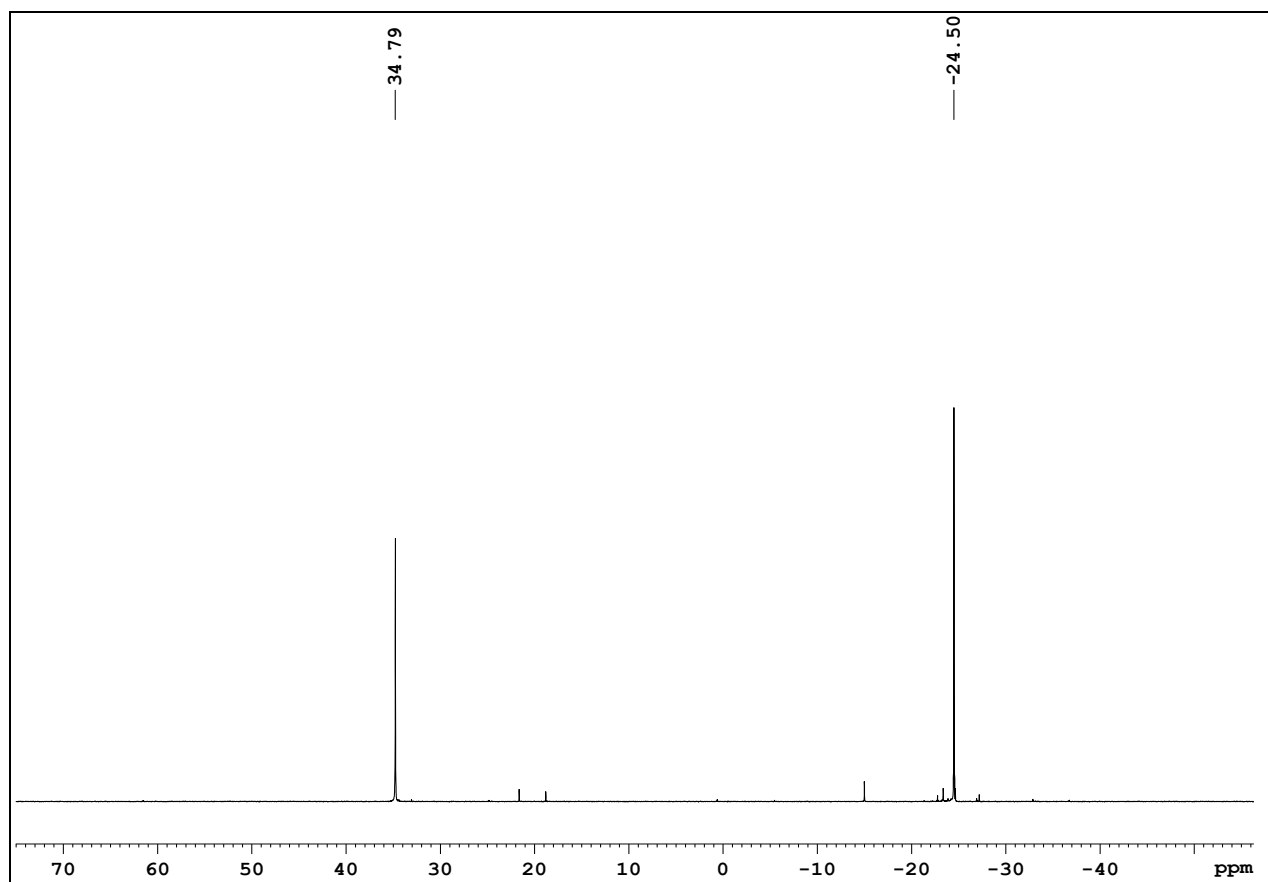


Figure S8. ^{31}P NMR Spectrum of L^3

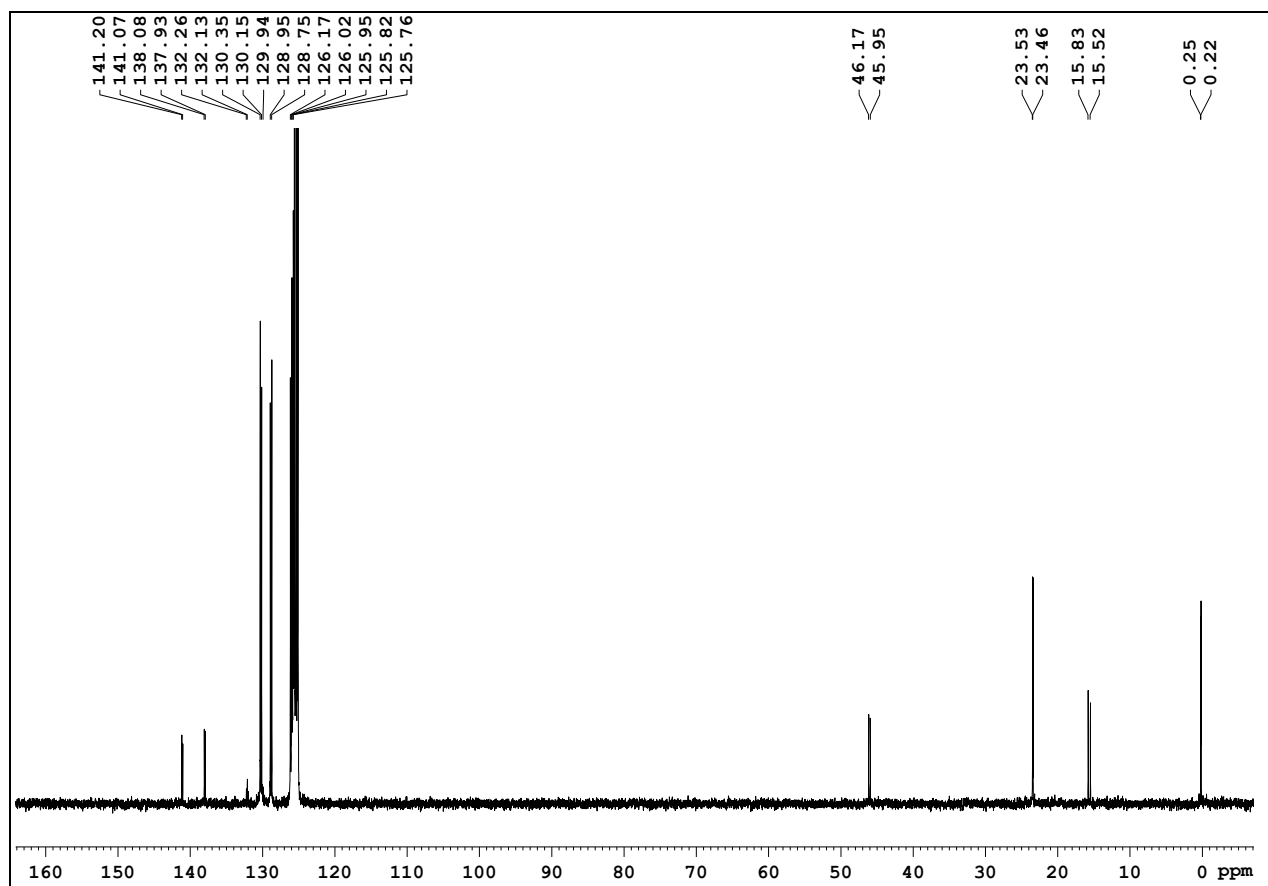


Figure S9. ¹³C NMR Spectrum of L^3

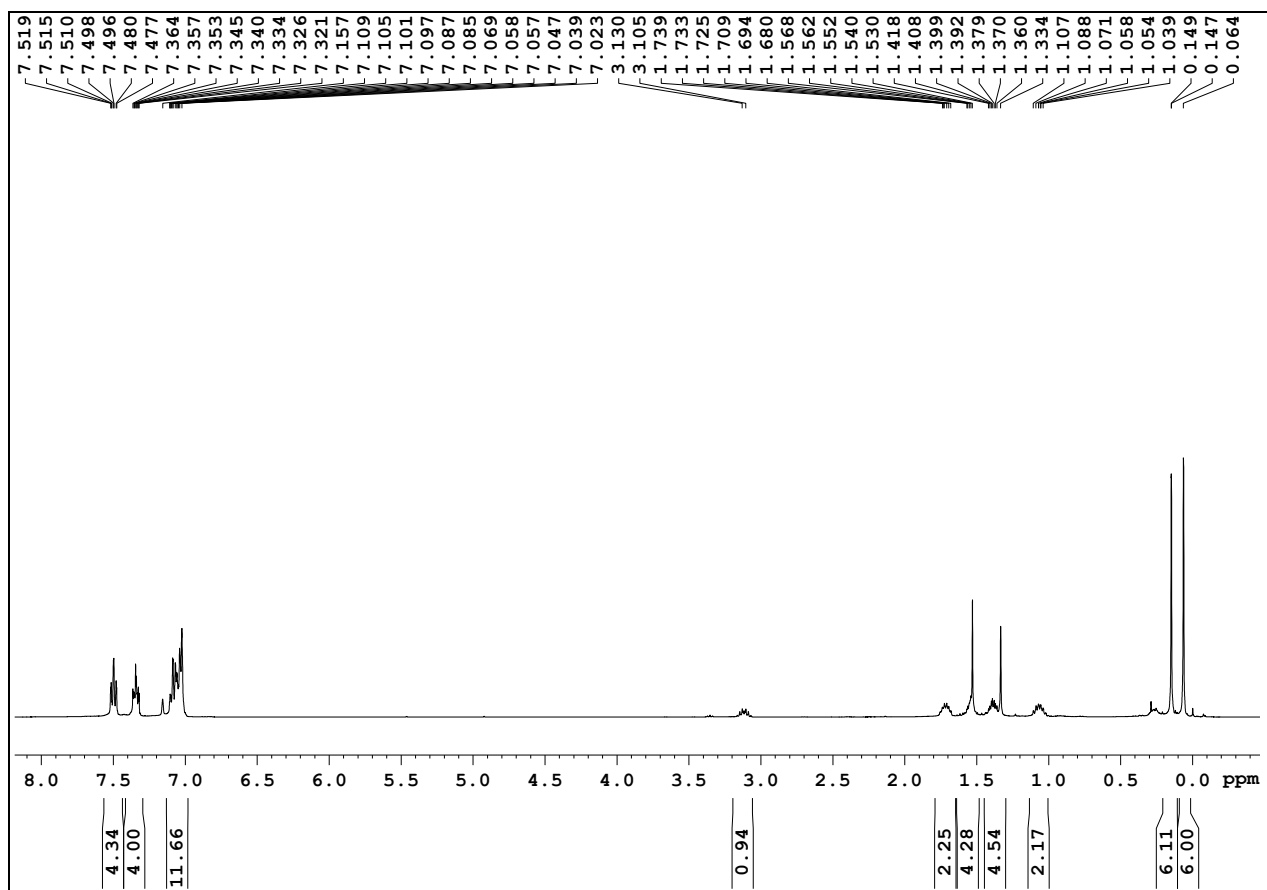


Figure S10. ^1H NMR Spectrum of L^4

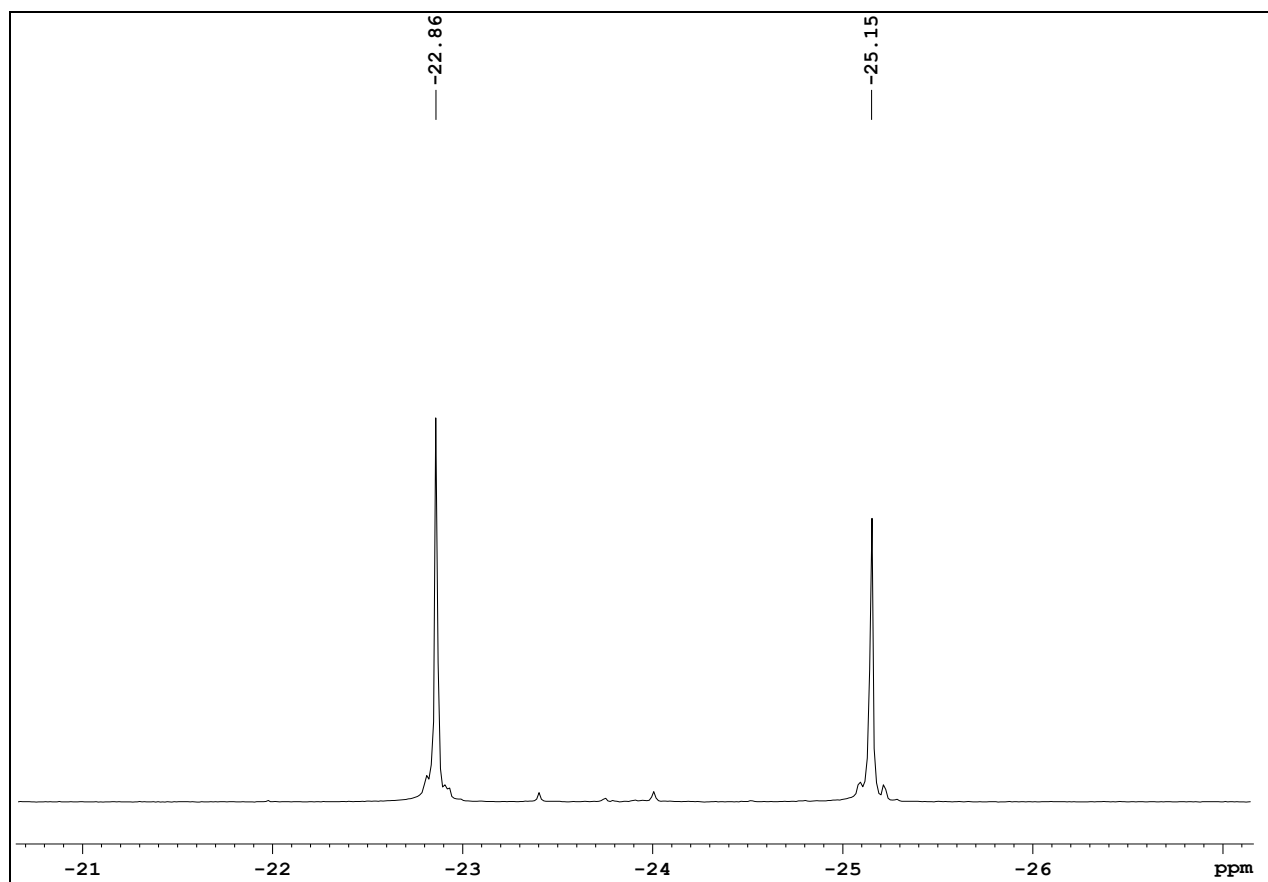


Figure S11. ^{31}P NMR Spectrum of L^4

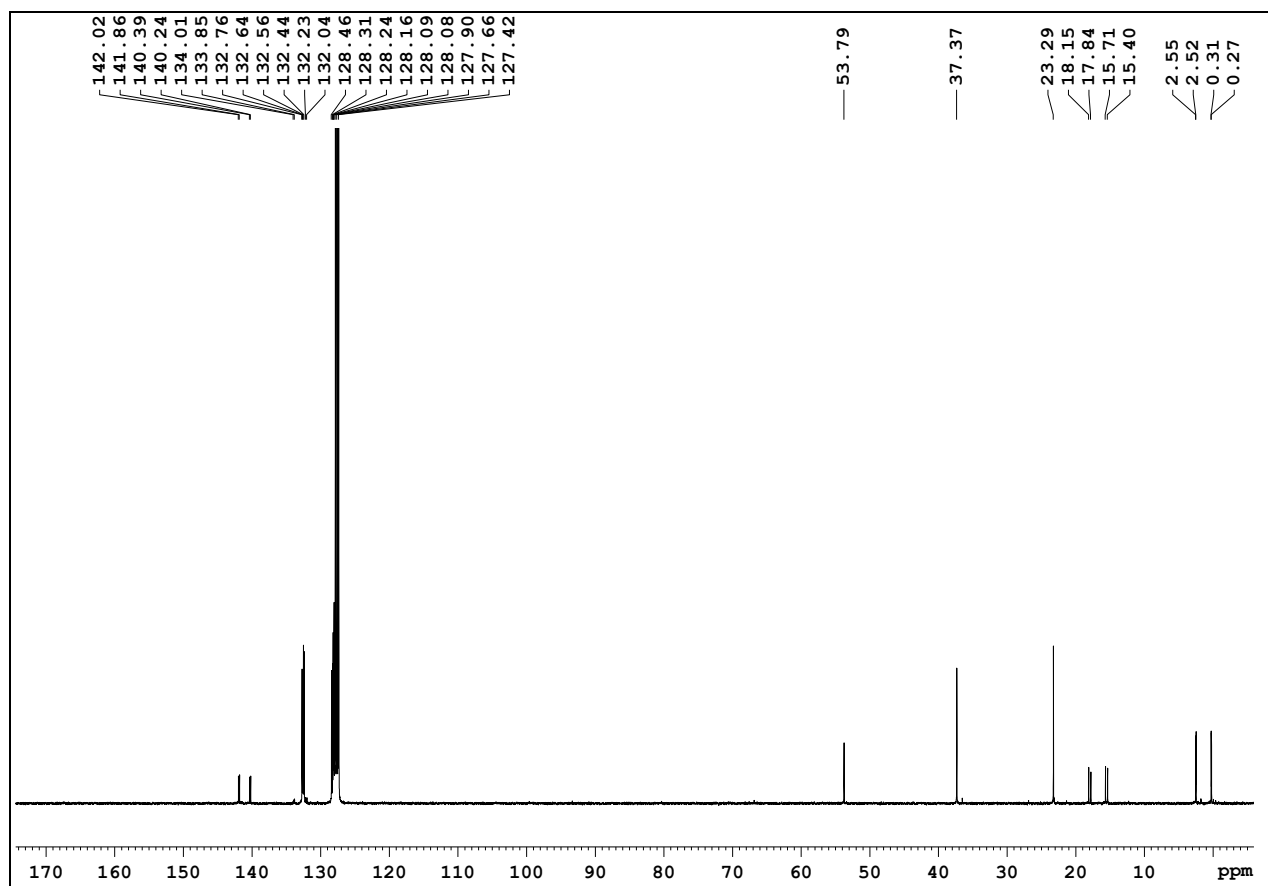


Figure S12. ¹³C NMR Spectrum of *L*⁴

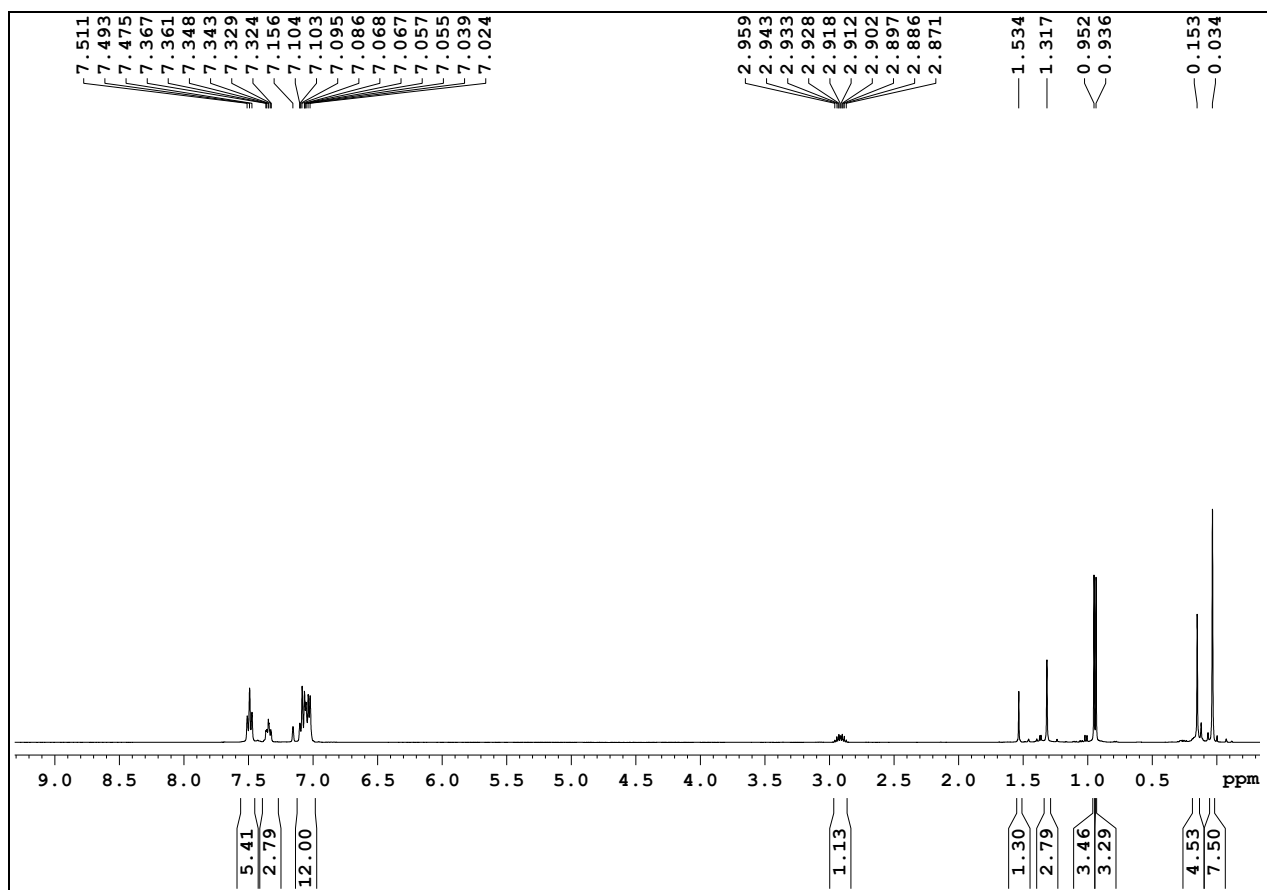


Figure S13. ^1H NMR Spectrum of L^5

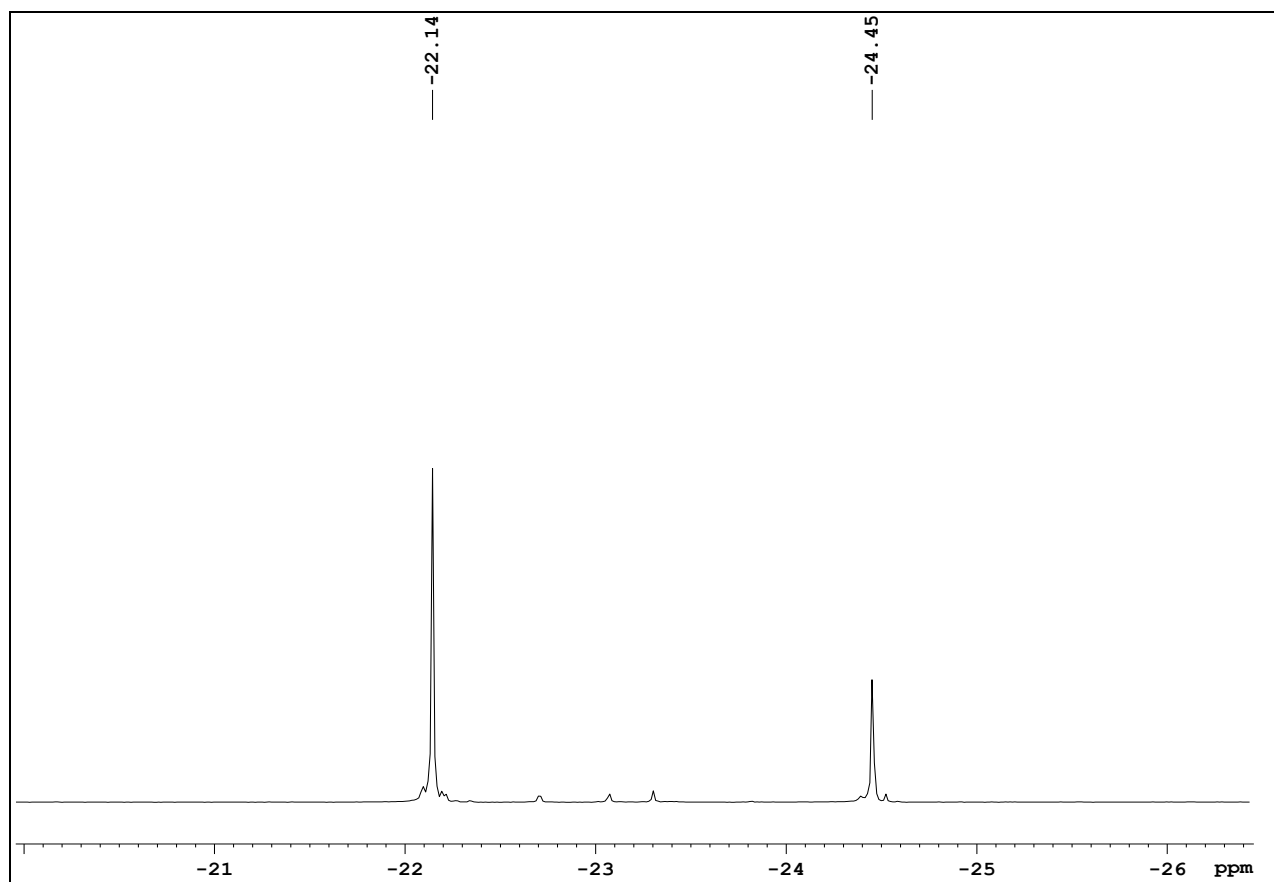


Figure S14. ^{31}P NMR Spectrum of L^5

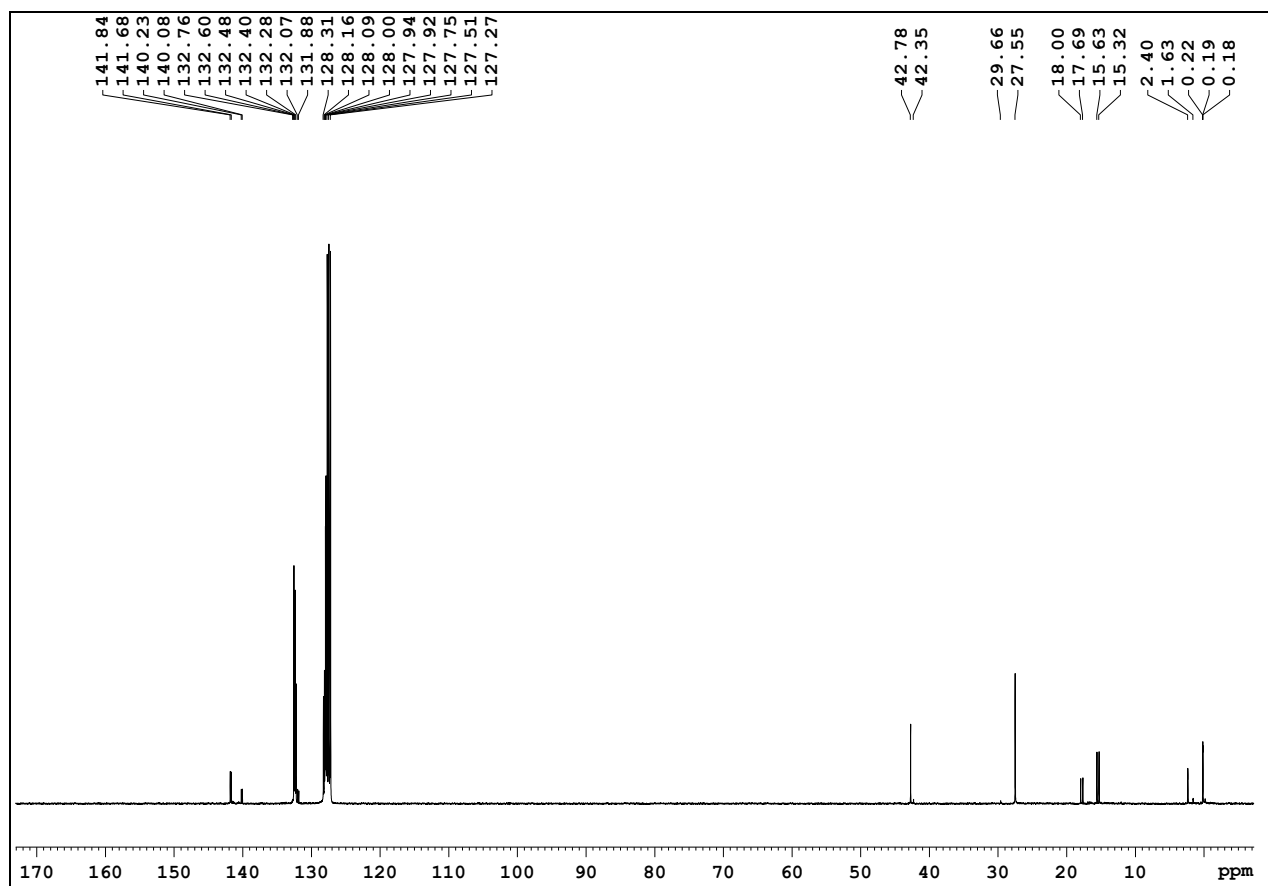


Figure S15. ^{13}C NMR Spectrum of L^5

3 Computational details

All DFT calculations for precatalyst **3** were carried out using Gaussian 09 package.³ Although M06L density functional was suggested as a suitable method for the detail investigation of oligomerization reactions.⁴ We further performed a benchmarking study to select a suitable method for complex **3** calculations. In addition to M06L,⁵ the free energy barriers of the rate-determining states of **path 1**, **path 2** and **path 3** were calculated using the ω B97X-D⁶ and B3LYP-D3⁷ functionals. The results show that the values of energy barriers calculated by the ω B97X-D and B3LYP-D3 functionals are very close to the M06L results (Table S1). The small difference in the free energy barriers shows that the reported results for the Cr complex are not sensitive to density functionals. Based on the previous study⁴ and our own findings, we decided to use M06L density functional for the evaluation of precatalyst **3**. In order to save computing time, the phenyl substitution on the phosphines in **L**³ has been replaced with methyl substituents.^{4, 8} Geometric optimization of stationary points and exploration of potential energy surfaces (PESs) were calculated without symmetry constraints by using M06L density functional,⁹ in combination with Stuttgart-Dresden (SDD) double- ζ valence basis set and effective core potential (ECP) for Cr (ECP10MDF)¹⁰ and 6-31G* basis set for all non-metal atoms.¹¹ The minimum energy crossing point (MECP) between the **62** and **42** surfaces was located using the methodology of Harvey¹² and sobMECP suite.¹³ The barrier for the spin-state crossing is derived from electronic energy ($E = -1668.2743$ a.u.) at the M06L level. The correction for solvent effect was calculated by using SMD¹⁴ solvation model for methylcyclohexane ($\epsilon = 2.024$). Thermal corrections were calculated at 298.15 K and 1 atm pressure with a harmonic approximation. In addition to 1 atm pressure, the effect of high pressure was also taken into consideration and the energy barriers of rate-determining states of

path 1, **path 2** and **path 3** were also calculated at 1MP (~ 10 atm) pressure. The lowering in the energy barrier of the rate-determining states of **path 2** at high pressure shows that high pressure promote double coordination of ethylene and 1-C₈ formation (Table S2). An ultrafine integration grid (99,590) was used throughout for numerical integrations. Important stages¹⁵ in the catalytic cycle, like ethylene coordination, oxidative coupling, metallacycle-ring extension and β -H elimination were investigated. Calculating the harmonic vibrational frequencies for optimized structures and noting the number of imaginary frequencies (IFs) made confirm the nature of all intermediates (no IF) and transition states (only one IF for each transition state). The latter was also made confirm via connecting reactants and products by intrinsic reaction coordinate (IRC) calculations. The spin multiplicities of all intermediates and transition states are marked in the main article.

Table S1. Evaluation of the Density Functionals for Benchmarking Study

Path	The Rate-determining States	Free Energy Barriers (kcal/mol)		
		M06L	ω B97X-D	B3LYP-D3
Path 1	5 \rightarrow TS_{6e,7}	13.7	14.1	15.9
Path 2	3b \rightarrow TS_{5',6a}	14.4	16.4	16.4
Path 3	5 \rightarrow TS_{5,9}	17.0	16.5	18.1

Table S2. Evaluation of the Effect of Pressure on the Energy Barriers of the Rate-determining States

Path	The Rate-determining States	Free Energy Barriers (kcal/mol)	
		Pressure=1 atm	Pressure=10 atm
Path 1	5 \rightarrow TS_{6e,7}	13.7	12.3
Path 2	3b \rightarrow TS_{5',6a}	14.4	11.7
Path 3	5 \rightarrow TS_{5,9}	17.0	17.0

4 X-ray Crystallographic Characterization

4.1 Characterization of single crystals

Single-crystals of X-ray quality were grown by slow diffusion of n-hexane into a concentrated CH₂Cl₂ solution of complex **6**. Bruker SMART APEX CCD diffractometer with graphite-monochromated Mo K- α radiations ($\lambda = 0.71073 \text{ \AA}$) was used to collect the crystallographic data at 113 K. Crystal class and unit cell parameters were obtained using SMART program package.¹⁶ Reflection data file was created by processing raw frame data using SAINT¹⁷ and SADABS.¹⁸ The structure was solved using the SHELXTL program and refined by full-matrix least squares method.¹⁹ The main crystallographic data are shown in Table S3. Further crystallographic information could be found in CIF file which is submitted to Cambridge Crystallographic Data Centre (CCDC), Cambridge, UK. The CCDC reference number for **6** was assigned as CCDC 1847128.

4.2 Structure description

The structure of the complex **6** was suggested in Figure S16. Additionally, one CH₂Cl₂ molecule was found with the complex **6** structure.

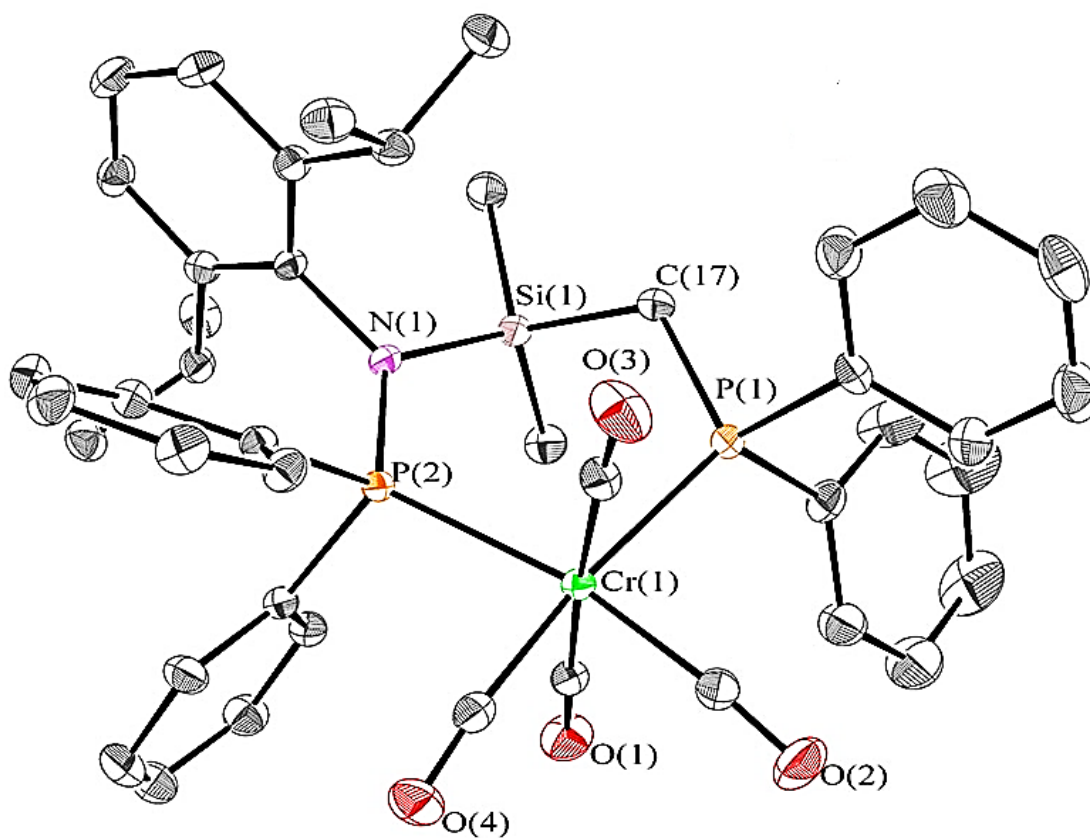


Figure S16. Molecular structure of Cr complex 6

Table S3. Crystallographic Determination Parameters for Complex **6**

Complex	6
Empirical formula	C ₄₄ H ₄₇ Cl ₂ CrNO ₄ P ₂ Si
Formula weight	866.75
Temperature	113 (2)K
Wavelength	0.71073 Å
Crystal system, space group	Triclinic, P-1
Unit cell dimensions	a = 9.801(2) Å; α = 87.32(3)° b = 10.711(2) Å; β = 78.54(3)° c = 22.081(4) Å; γ = 72.00(3)°
Volume	2160.4(7) Å ³
Z, Calculated density	2, 1.331 Mg/m ³
Absorption coefficient	0.532 mm ⁻¹
F(000)	902
Theta range for data collection	1.88 to 27.84°
Limiting indices	-12 ≤ h ≤ 12, -14 ≤ k ≤ 14, -28 ≤ l ≤ 28
Reflections collected / unique	25725 / 10181 [R(int) = 0.0348]
Completeness to theta = 27.84	99.4%
Refinement method	Full-matrix least-squares on F ²
Data / restraints / parameters	10181 / 0 / 502
Goodness-of-fit on F ²	1.080
Final R indices [I > 2sigma(I)]	R1 = 0.0451, wR2 = 0.1199
R indices (all data)	R1 = 0.0531, wR2 = 0.1294
Largest diff. peak and hole	0.805 and -0.893 e·Å ⁻³

5 References

(1) Boulens, P.; Pellier, E.; Jeanneau, E.; Reek, J. N.; Olivier-Bourbigou, H.; Breuil, P.-A. R. Self-Assembled Organometallic Nickel Complexes as Catalysts for Selective Dimerization of Ethylene into 1-Butene. *Organometallics* **2015**, *34*, 1139-1142.

- (2) (a) Schore, N. E.; Benner, L. S.; LaBelle, B. E. Indirect Metal-Metal Linkage: Cyclic Ferrocene Complexes with a Second Metal Linked via Remote Phosphine Functionality. *Inorg. Chem.* **1981**, *20*, 3200-3208. (b) Holmes-Smith, R. D.; Osei, R. D.; Stobart, S. R. Phosphinoalkylsilanes: Synthesis and Spectroscopic Properties of Phosphino(silyl)methanes, 1-Phosphino-2-Silylethanes, and 1-Phosphino-3-Silylpropanes. *J. Chem. Soc., Perkin Trans. 1* **1983**, 861-866. (c) Fraenkel, G.; Winchester, W. R.; Williard, P. Lithio(diphenylphosphino)methane-Tetramethylethylenediamine: Crystal Structure and NMR Studies of a Coordinatively Unsaturated, Monomeric Organolithium. *Organometallics* **1989**, *8*, 2308-2311.
- (3) Frisch, M.; Trucks, G.; Schlegel, H.; Scuseria, G.; Robb, M.; Cheeseman, J.; Scalmani, G.; Barone, V.; Mennucci, B.; Petersson, G. GAUSSIAN09. Revision D. 01. Gaussian Inc., Wallingford, CT, USA. **2013**.
- (4) McGuinness, D. S.; Chan, B.; Britovsek, G. J.; Yates, B. F. Ethylene Trimerisation with Cr-PNP Catalysts: A Theoretical Benchmarking Study and Assessment of Catalyst Oxidation State. *Aust. J. Chem.* **2014**, *67*, 1481-1490.
- (5) (a) Zhao, Y.; Truhlar, D. G. The M06 Suite of Density Functionals for Main Group Thermochemistry, Thermochemical Kinetics, Noncovalent Interactions, Excited States, and Transition Elements: Two New Functionals and Systematic Testing of Four M06-Class Functionals and 12 other Functionals. *Theor. Chem. Acc.* **2008**, *120*, 215-241. (b) Zhao, Y.; Truhlar, D. G. Density Functionals with Broad Applicability in Chemistry. *Acc. Chem. Res.* **2008**, *41*, 157-167.
- (6) (a) Chai, J.-D.; Head-Gordon, M. Systematic Optimization of Long-Range Corrected Hybrid Density Functionals. *J. Chem. Phys.* **2008**, *128*, 084106. (b) Chai, J.-D.; Head-Gordon, M. Long-

Range Corrected Hybrid Density Functionals with Damped Atom-Atom Dispersion Corrections. *Phys. Chem. Chem. Phys.* **2008**, *10*, 6615-6620.

(7) (a) Becke, A. D. Density-functional thermochemistry. III. The Role of Exact Exchange. *J. Chem. Phys.* **1993**, *98*, 5648-5652. (b) Chengteh, L.; Weitao, Y.; Parr, R. Development of the Colle-Salvetti Correlation-Energy Formula into a Functional of the Electron Density. *Phys. Rev. B* **1988**, *37*, 785-789. (c) Goerigk, L.; Hansen, A.; Bauer, C.; Ehrlich, S.; Najibi, A.; Grimme, S. A Look at the Density Functional Theory zoo with the Advanced GMTKN55 Database for General Main Group Thermochemistry, Kinetics and Noncovalent Interactions. *Phys. Chem. Chem. Phys.* **2017**, *19*, 32184-32215.

(8) Britovsek, G. J.; McGuinness, D. S.; Wierenga, T. S.; Young, C. T. Single- and Double-Coordination Mechanism in Ethylene Tri- and Tetramerization with Cr/PNP Catalysts. *ACS Catal.* **2015**, *5*, 4152-4166.

(9) Zhao, Y.; Truhlar, D. G. A New Local Density Functional for Main-Group Thermochemistry, Transition Metal Bonding, Thermochemical Kinetics, and Noncovalent Interactions. *J. Chem. Phys.* **2006**, *125*, 194101.

(10) (a) Andrae, D.; Haeussermann, U.; Dolg, M.; Stoll, H.; Preuss, H. Energy-Adjusted Ab Initio Pseudopotentials for the Second and Third Row Transition Elements. *Theor. Chim. Acta.* **1990**, *77*, 123-141. (b) Martin, J. M.; Sundermann, A. Correlation Consistent Valence Basis Sets for Use with the Stuttgart-Dresden-Bonn Relativistic Effective Core Potentials: The Atoms Ga-Kr and In-Xe. *J. Chem. Phys.* **2001**, *114*, 3408-3420.

(11) (a) Hehre, W. J.; Ditchfield, R.; Pople, J. A. Self-Consistent Molecular Orbital Methods. XII. Further Extensions of Gaussian-Type Basis Sets for Use in Molecular Orbital Studies of Organic Molecules. *J. Chem. Phys.* **1972**, *56*, 2257-2261. (b) Hariharan, P. C.; Pople, J. A. The

Influence of Polarization Functions on Molecular Orbital Hydrogenation Energies. *Theor. Chim. Acta.* **1973**, 28, 213-222. (c) Krishnan, R.; Binkley, J. S.; Seeger, R.; Pople, J. A. Self-Consistent Molecular Orbital Methods. XX. A Basis Set for Correlated Wave Functions. *J. Chem. Phys.* **1980**, 72, 650-654.

(12) Harvey, J. N.; Aschi, M.; Schwarz, H.; Koch, W. The Singlet and Triplet States of Phenyl Cation. A Hybrid Approach for Locating Minimum Energy Crossing Points Between Non-Interacting Potential Energy Surfaces. *Theor. Chem. Acc.* **1998**, 99, 95-99.

(13) (a) Lu, T.; Chen, F. Multiwfn: A Multifunctional Wavefunction Analyzer. *J. Comput. Chem.* **2012**, 33, 580-592. (b) Harvey, J. N.; Aschi, M. Spin-Forbidden Dehydrogenation of Methoxy Cation: A Statistical View. *Phys. Chem. Chem. Phys.* **1999**, 1, 5555-5563.

(14) Marenich, A. V.; Cramer, C. J.; Truhlar, D. G. Universal Solvation Model Based on Solute Electron Density and on a Continuum Model of the Solvent Defined by the Bulk Dielectric Constant and Atomic Surface Tensions. *J. Phys. Chem. B.* **2009**, 113, 6378-6396.

(15) (a) Briggs, J. R. The Selective Trimerization of Ethylene to Hex-1-ene. *J. Chem. Soc., Chem. Commun.* **1989**, 674-675. (b) Arteaga-Müller, R.; Tsurugi, H.; Saito, T.; Yanagawa, M.; Oda, S.; Mashima, K. New Tantalum Ligand-Free Catalyst System for Highly Selective Trimerization of Ethylene Affording 1-Hexene: New Evidence of a Metallacycle Mechanism. *J. Am. Chem. Soc.* **2009**, 131, 5370-5371. (c) Epshteyn, A.; Trunkely, E. F.; Kissounko, D. A.; Fettinger, J. C.; Sita, L. R. Experimental Modeling of Selective Alkene Oligomerization: Evidence for Facile Metallacyclopentane Dehydrogenation Mediated by a Transannular β -Hydrogen Agostic Interaction. *Organometallics* **2009**, 28, 2520-2526.

(16) SMART Software Users Guide, Version 4.21; Bruker AXS, Inc.; Madison, WI, **1997**

(17) SAINT, Version 6.45; Bruker AXS, Inc.; Madison, WI **2003**.

(18) Sheldrick, G. M. SADABS, Version 2.10; Bruker AXS, Inc.

(19) Sheldrick, G. M. Acta Cryst. A64, **2008**, 112-122.